Albumin as a probe for clathrin-independent endocytosis and transcytosis into experimental brain metastases of breast cancer.

Imran Khan[1], Brunilde Gril[1#], Anurag Paranjape[1*], Christina Burks[2], Christina Robinson[3], Simone Difilippantonio[3], Wojciech Biernat[4], Michał Bieńkowski[4], Rafał Pęksa[4], Renata Duchnowska[5], Jacek Jassem[6], Priscilla K. Brastianos[7], Philippe Metellus[8], Emilie Bialecki[8], Carolyn C. Woodroofe[9], Haitao Wu[9], Rolf Swenson[9], Patricia S. Steeg[1$]

1. Women's Malignancies Branch, Center for Cancer Research, National Cancer Institute, Bethesda, MD

2. Electron Microscopy Laboratory, Cancer Research Technology Program, Leidos Biomedical Research, Inc., Frederick National Laboratory for Cancer Research (FNLCR), Frederick MD.

3. Laboratory Animal Sciences Program, Frederick National Laboratory for Cancer Research (FNLCR), Frederick, MD.

4. Department of Pathology, Medical University of Gdańsk, 7 Dębinki St, 80-211, Gdańsk, Poland.

5. Department of Oncology, Military Institute of Medicine, Warsaw, Poland.

6. Department of Oncology and Radiotherapy, Medical University of Gdańsk, Poland.

7. Division of Neuro-Oncology, Massachusetts General Hospital Cancer Center, Harvard Medical School, Boston, MA.

8. Ramsay Général de Santé, Hôpital Privé Clairval, Département de Neurochirurgie and Aix-Marseille Université, Institut de Neurophysiopathologie – UMR 7051, Marseille, France.

9. Chemistry and Synthesis Center, National Heart, Lung and Blood Institute, NIH, Bethesda, MD.

Running title: Albumin transcytosis in brain metastasis

$ Corresponding Author: Patricia S. Steeg, steegp@mail.nih.gov, Building 37, Room 1126, NCI, NIH, Bethesda MD 20892 USA

Current address: Tumor Metastasis Branch, Division of Cancer Biology, National Cancer Institute, National Institutes of Health, 9609 Medical Center Drive, Rockville, MD 20850-9745

* Current address: UPMC Center for Ultrasound Molecular Imaging and Therapeutics, University of Pittsburgh, 3550 Terrace St, Pittsburgh, PA 15213

Conflict of Interest: None

Word Count: 6351. Six figures.

Abstract

Background: Improvements in drug delivery to brain metastases are needed. We hypothesized that albumin transcytosis would demonstrate widespread distribution in experimental brain metastases of breast cancer.

Methods: The metastatic and uninvolved brain localization of five transcytotic pathways was determined in two hematogenous models of breast cancer brain metastasis. Albumin was compared to distribution of a Biocytin-TMR, which uses paracellular permeability. An *in vitro* model for transcytosis of albumin across a blood-tumor barrier (BTB) was developed and characterized for modes of endocytosis. Human craniotomy specimens were stained for endocytic proteins.

Results: Albumin transcytosis occurred in virtually all metastases, including micrometastases; distribution was greater than, and independent of paracellular permeability. Albumin uptake into the normal brain parenchyma was negligible. Using an *in vitro* assay that permits albumin transcytosis through a BTB, albumin used a form of macropinocytosis with features of clathrin-independent endocytosis (CIE), involving the neonatal Fc receptor (FcRn), Galectin-3 and membrane sphingolipids. Human craniotomy specimens demonstrated FcRn and Galectin-3 staining.

Conclusions: The data identify CIE as a pathway with optimal features for drug delivery into brain metastases.

Keywords: Brain metastasis, transcytosis, albumin, blood-tumor barrier

Key Points:

- Albumin transcytosis occurred in virtually all experimental brain metastases in two model systems.
- Albumin transcytosis occurred independently of paracellular permeability.
- Albumin transcytosis uses a clathrin-independent endocytosis pathway.

Importance of the Study: Improvements in drug delivery to brain metastases are needed to enhance therapeutic efficacy. We report that labeled albumin has a distribution pattern in two

models of experimental brain metastases of breast cancer that may be optimal for translational development: Albumin transcytosis occurred in nearly all lesions, including micrometastases, and was independent of paracellular permeability. Using an *in vitro* model of the blood-tumor barrier, we found that albumin uses a clathrin-independent endocytic pathway requiring FcRn and galectin-3. Human craniotomy specimens stained for both proteins, demonstrating that the pathway can be operative in the human. A CIE pathway may represent an advantageous mechanism for linkage to drugs for brain metastasis therapy.

Introduction

Brain (CNS) metastases of breast and lung cancers and melanoma confer serious physical and neurocognitive effects and contribute to patients' deaths[1]. Most cytotoxic drugs, including those with known systemic activity in the metastatic setting, do not fully penetrate an intact BBB and have limited activity in CNS malignancies [2,3]. In HER2-positive breast cancer, antibody-drug conjugates and new small-molecule tyrosine kinase inhibitors, including combinations with neratinib or tucatinib, confer increased progression free survival[4-6]. New approaches to drug delivery to brain metastases are still needed.

Drug distribution to brain metastases is complex, involving standard variables such as uptake, clearance, and edema, but a unique contributor is the blood-brain barrier (BBB). When a tumor forms in the brain, tumor cells often colonize on the outside of the BBB, which is now described as a blood-tumor barrier (BTB)[7]. Low and heterogeneous drug levels in hematogenously derived brain metastases were reported for drugs and markers[8-13]. For paclitaxel, approximately 85% of brain lesions had greater drug distribution than uninvolved brain, yet only the 10% of lesions with the highest uptake showed apoptosis in response to drug[11]. Most BTB permeability in these studies is paracellular, resulting from breakage of the tight- and adherens junctions linking endothelial cells in the BBB, so that drug can diffuse between endothelial cells into the brain[7].

We have now focused on transcytosis as a potential mechanism of drug permeability for breast cancer experimental brain metastases. Transcytosis is a complex series of mechanisms for the intracellular transport of macromolecules within membrane-bound vesicles. In the normal BBB needednutrients enter via multiple transcytotic pathways, including receptor-mediated transport, carrier-mediated transport, lipid transport, lipid diffusion and, to a limited extent, macropinocytosis of soluble compounds (rev. in[7]). Transcytotic pathways vary in initial modes of cell membrane endocytosis and the intracellular fate of vesicles. For various CNS diseases, ligands to transcytotic pathways such as the transferrin receptor (TfR) have been linked to a number of potential drugs or used to coat nanoparticles (rev. in[14]), demonstrating the intent for translation of these pathways. However, most of these studies use normal brain as an endpoint for permeability experiments, and the relationship of transcytotic pathways to brain metastases is inadequately understood. Angiopep, a peptide derived from low density lipoprotein receptor

related protein 1 (LRP1), also uses transcytosis. A clinical trial of Angiopep conjugated to paclitaxel showed some disease benefit but the trial did not meet its primary endpoint[15].

Herein we have focused on albumin as a transcytotic pathway of interest based on preliminary experiments identifying a widespread metastatic distribution pattern among five well known transcytosis ligands. Albumin is a major constituent of blood. It has been reported to use vesicles to move into the normal BBB [16,17] where it is then recycled back to the bloodstream. Interestingly, in a time course of another BBB disruption, experimental ischemic stroke, an initial rapid increase in BBB permeability to Alexa-Albumin by transcytosis was observed, followed by increased paracellular permeability of biocytin[18].

Herein, we hypothesize that albumin transcytosis is elevated in brain metastases. We demonstrate its consistent permeation into brain metastases, including micrometastases. Albumin transcytosis was independent of a paracellular permeability marker. To further study its transcytotic mechanism, we developed an *in vitro* BTB assay that demonstrated both paracellular permeability and transcytosis comparable to *in vivo* data. Albumin used a form of macropinocytosis termed clathrin-independent endocytosis (CIE) involving its binding to the neonatal Fc receptor (FcRn) and coalescence for endocytosis via Galectin-3 (Gal-3) and sphingolipids. These data identify a CIE pathway for transcytosis with high specificity for brain metastases, which may facilitate the development of improved drug delivery of compounds.

Materials and Methods

Cell line origins and authentication. The origins and validation of the triple-negative 231-BR[19] and the HER2-overexpressing JIMT1-BR[20] are previously reported (see Supplementary methods). For *in vitro* BBB and BTB assays, immortalized human astrocytes (HAL) and pericytes (HPL) were generated using SV40 Large T antigen [21]. The mouse brain endothelial line bEnd.3 was used. Culture conditions are listed in Supplementary Methods.

Animal Experiments- General Information. All animal experiments were performed under the regulation of the Animal Care and Use Committee (ACUC) of the National Cancer Institute (NCI). Five-seven week old female athymic NIH nu/nu mice were injected in the left cardiac ventricle with 1.75 x 10^5 231-BR or JIMT1-BR cells as described, with metastasis formation in 3-4 weeks[20]. Microscopic analysis of brain sections quantified the number and types of lesions, and probe distribution. Metastatic colonies were defined as grouped nests of tumor cells that would coalesce into a single large lesion if the mice were not sacrificed for a humane endpoint. Micrometastases were defined as single tumor cells or a group of a few tumor cells distant from a metastatic colony. Further details are in Supplemental Methods.

Comparison of five transcytosis ligands. Five known transcytosis ligands, similarly labeled, were compared for distribution to metastases *in vivo*. After the development of brain metastases and on the day of necropsy, mice were injected iv with a far-red fluorescent probe of either albumin, cationic albumin, transferrin peptide, LRP-1 peptide or folic acid peptide; the probes circulated for a short (30 min-1h) or longer (4-6h) period, followed by perfusion. All metastatic colonies in one section per mouse brain were assigned to an expression pattern fitting its maximal distribution, as listed on Figure 1B. The normal brains of three uninjected mice per arm were also analyzed for transcytosis of each probe by these same criteria.

Comparison of transcytosis versus paracellular permeability: 231-BR and JIMT1-BR cells were injected into mice and developed brain metastases. After brain metastasis formation and on the day of necropsy Far-red-Albumin (Alexa Fluor™ 647-albumin) and Biocytin-TMR was injected (iv) and circulated for 60 and10 min, respectively, followed by the perfusion. Whole brain sections were scanned for fluorescence or H&E staining using a Zeiss AxioScan.Z1 Slide Scanner. All metastatic colonies and micrometastases were evaluated for the extent of albumin and biocytin distribution into categories listed on Figure 2. For the metastatic

colonies, distribution was further categorized into paravascular (around capillaries) and diffuse (throughout the lesion) distribution patterns.

Electron microscopy: Nu/nu mice bearing JIMT1-BR brain metastases were obtained as described above and compared to six uninjected mice (sham). Metastases were manually dissected and processed for electron microscopy, as were samples of normal brain (Supplementary methods). Samples were processed and analyzed by the Electron Microscopy Laboratory, Leidos Biomedical Research, Inc. as described in Supplementary Methods.

***In vitro* blood-brain barrier (BBB) and blood-tumor barrier (BTB) assays.** The *in vitro* BBB/BTB assays reflecting paracellular permeability was previously established[21] in 24-well plates with transwell inserts. Herein, inserts with 0.4 µm (Corning, #353095) and 3 µm pores (Corning, #353096) were tested. Albumin endocytosis and transcytosis was evaluated by addition of 50 µg/ml Alexa Fluor™ 594-albumin or Alexa Fluor™ 488-albumin to the top of the assay, and culture for 30 min. Endpoints included (1) endocytosis within endothelial cells, (2) albumin transcytosis to the lower fluid compartment, and (3) albumin transcytosis and uptake into astrocytes in the lower compartment (see Supplementary methods). For inhibitor studies, after establishment of BBB/BTB endothelial cells were serum deprived for 1 hour in Opti-MEM. Cells were pre-treated with inhibitors for 30 min at nontoxic concentrations (see Supplementary methods).

shRNA-mediated knockdown of endothelial clathrin-independent endocytosis (CIE) genes. shRNA knockdown of genes associated with CIE was performed in bEnd.3 cells as described in Supplementary methods.

Glycoprotein Isolation. Glycoproteins were isolated using a glycoprotein isolation kit (89804; Thermo Fisher Scientific) as per the manufacturer's protocol. 50 µg of proteins were loaded on SDS PAGE gel for assessing the level of FcRn and SPARC glycosylation using their antibodies.

Co-immunoprecipitation (Co-IP). Protein–protein interactions between Galectin-3 and FcRn were studied using Co-Immunoprecipitation Kit (ab206996, Abcam) (see Supplementary methods).

Colocalization using confocal microscopy. Mouse bEnd.3 endothelial cells were cultured in chamber slides and stained by immunofluorescence for FcRn or Galectin-3 as described in Supplementary methods. Confocal microscopy was used to visualize staining.

Immufluorescence (IF) of frozen human brain metastasis specimens. IF staining was performed as described previsouly[19] on flash frozen human brain metastasis craniotomy specimens, collected under approved protocols (see Supplementary Methods).

Immunohistochemistry (IHC) of human brain metastasis specimens. Formalin-fixed, paraffin embedded blocks of human craniotomy specimens were collected as described in Supplementary methods. All procedures were performed according to the manufacturer's instructions (LifeSpan, Inc.). The immunoreactivity was scored semi-quantitatively on a 0-3+ intensity basis in the endothelial, cancer, and brain parenchymal compartments.

Graphic representation and statistical analysis. See Supplementary methods.

Results

Far-red albumin exhibits a widespread distribution in experimental brain metastases. Far-red emitting fluorescent labeled ligands/proteins for five well-known CNS transcytosis pathways were analyzed *in vivo* to identify those with the highest distribution pattern in brain metastases. Mice bearing either 231-BR or JIMT1-BR metastases were injected iv with Far-red labeled albumin, cationic albumin, LRP-1 receptor peptide, transferrin peptide or folic acid peptide; each probe was circulated for a short (30 min-1h) or long (4-6h) period, at which time mice were perfused to remove probe from the bloodstream (Figure 1A). Brain sections were analyzed by confocal microscopy for the maximal extent of distribution in metastatic colonies and uninvolved brain; a similar experiment was performed on uninjected mice. Representative images of the most abundant pattern of probe distribution in the JIMT1-BR model system, and a tabulation of the percentage of metastatic colonies with each class of probe distribution are shown on Supplementary Figures 1-2 and Figure 1B. The probe with the most widespread metastatic distribution was albumin. The "diffuse" category of albumin distribution (Figure 1B-D), including perivascular distribution and a cloud of diffuse ligand expression covering much of the lesion, increased from 9.2% to 32.4% of metastatic colonies with time of circulation in the 231-BR model, and from 21.1% to 28.6% of metastatic colonies in the JIMT1-BR model system. This pattern is hypothesized to be optimal for drug delivery to most tumor cells. At short circulation times, albumin was localized in intracellular vesicles in the capillary space (Figure 1E). Co-localization of albumin to tumor cells was widespread (Figure 1F). Uninvolved brain parenchyma was rarely positive. In the normal brain, albumin was distributed only within endothelial cells at 1h and largely absent at 6h (Figure 1B), consistent with the known endocytic and recycling role of the endothelial neonatal Fc receptor (FcRn) (rev. in[22]). Distribution of Far-red-Dye control was absent in the normal brain and predominantly faint in the metastatic models. The data point to widespread, stable distribution of albumin in metastases over the 6h experimental period, with relatively little normal or uninvolved brain penetration.

Albumin transcytosis is distinct from paracellular marker distribution. To provide a comparison of paracellular and transcytotic BTB pathways, mice with 231-BR or JIMT1-BR brain metastases were dosed iv with Far-red-Albumin (Albumin-Alexa Fluor^{TM} 647) and Biocytin TMR (Tetramethylrhodamine Biocytin), a compound of approximate drug size (869 Da) used as a probe of paracellular permeability[18,23], before perfusion and necropsy.

Translational questions addressed by this experiment were: (1) if albumin distribution occurred in both large and micrometastases, and (2) could albumin reach metastases impermeable to a paracellular permeability marker.

Figure 2A demonstrates the colocalization of metastases and Far-red albumin. Albumin distribution was determined in 252 231-BR and 301 JIMT1-BR metastases. Micrometastases outnumbered metastatic colonies by approximately 2-fold in both models. Albumin was visible in 97.6% and 96.4% of 231-BR metastatic colonies and micrometastases, respectively, and all JIMT1-BR metastases (Figure 2B). For the metastatic colonies, positive distribution was scored as "paravascular", an albumin+ area around the capillary, or "diffuse" throughout the lesion. Diffuse albumin distribution was observed in the majority of metastatic colonies, 64.3% of 231-BR and 87.4% of JIMT1-BR lesions (Figure 2C); paravascular albumin expression was observed in 32.1% and 12.6% of the metastases, respectively.

For a comparison of albumin and biocytin distribution, metastases were separated into metastatic colonies and micrometastases; each category was further separated into an expression pattern: No uptake; biocytin only; albumin only (representative examples, Figure 2D); both biocytin and albumin, with biocytin more prominent; both compounds with albumin more prominent (Example, Figure 2D). Where both compounds were detected but albumin > biocytin, the difference in expression levels was remarkable with albumin bright and biocytin barely detectable. For the 231-BR and JIMT1-BR models, metastatic colonies were predominately albumin > biocytin (65.5% and 78.2%, respectively) with 30.9% and 21.6% albumin only distribution, respectively. Biocytin-only expression was not observed and biocytin>albumin constituted <2% of lesions (Figure 2E and Supplementary Figure 3). Micrometastases of 231-BR and JIMT1-BR were predominately albumin-only (73.8% and 74.8%, respectively), with albumin > biocytin constituting most of the remaining lesions (23.8% and 24.8%, respectively) (Figure 2F). Biocytin only expression was not observed and biocytin > albumin constituted < 1% of micrometastases.

Development of an *in vitro* BBB and BTB model system incorporating albumin transcytosis. We previously reported an *in vitro* model system for paracellular distribution of compounds through a BBB or BTB[21]. Briefly, brain endothelial cells were cultured to confluence on the top side of a 0.4 µm porous filter, with pericytes cultured on the bottom side. The insert was then placed in a chamber containing astrocytes in culture medium, with (BTB) or without

(BBB) tumor cells. This model faithfully reflected Texas red dextran paracellular permeability *in vivo*[24]. When Albumin-Alexa Fluor™ 594 was applied to this configuration, no endocytosis or transcytosis was observed. After many modifications, revision of one feature enabled transcytosis. Albumin endocytosis into endothelial cells was observed only with wider, 3.0 µm pores (Figure 3A-B and Supplementary Figure 4A-B). Confocal microscopy through the width of the 3.0 µm porous filter showed that cell processes from phalloidin/NG2 stained pericytes invaded through these larger pores to establish connections with the endothelium (Figure 3C), similar to their peg-and-socket physical interaction in the normal BBB[25]. Transcytosis was confirmed in the 3.0 µm cultures by albumin distribution into culture medium in the lower chamber (Figure 3D and Supplementary Figure 4C). Paracellular distribution of doxorubicin was slightly higher in BTB than BBB cultures but was unaffected by pore size (Figure 3E). Both 231-BR and JIMT1-BR tumor cells promoted endothelial endocytosis of albumin in vesicles that costained with Rab11 (Figure 3F-H) and transcytosis into astrocytes in the lower chamber (Figure 3I).

Albumin transcytosis by macropinocytosis, but dependent on FcRn. We investigated the endocytic process by which albumin penetrates endothelia. Incubation of *in vitro* BTB cultures with Fillipin III or Chlorpromazine, inhibitors of caveolin-dependent[26] and clathrin-dependent[27], endocytosis, respectively, had no significant effect on albumin endocytosis. Ethylisopropylamiloride, (EIPA), an inhibitor of macropinocytosis[28], inhibited albumin endocytosis by 80.3% ($p<0.0001$) in 231-BR cells and (Figure 4A, C) and 95.5% ($p<0.0001$) in JIMT1-BR cells (Figure 4B, D). Macropinocytosis, translated as “big drinking”, is the intake of fluid and soluble constituents in large vesicles. As a nonselective process, however, fluid and whatever is dissolved in it is taken up in classical macropinocytosis. It would make little sense that drugs would not be similarly taken up and readily distributed to brain metastases, in contrast to voluminous experimental data.

A potential answer to this conundrum lies within the general category of macropinocytosis: A protein-binding macropinocytotic pathway has been described, termed clathrin-independent endocytosis (CIE), also known as clathrin-independent carrier (CLIC), glycolipid and lectin hypothesis (GL-Lec), or GPI-enriched compartment (GEEC). As an example, the membrane protein CD44, via extracellular N-glycosylation, binds galectin 3 (Gal-3) which, via its pentamerization, coalesces multiple CD44 proteins. When coalesced in a

membrane region containing high levels of glycosphingolipids, an endocytic pit forms[29]. If this mechanism were to apply to albumin, it must bind an endothelial membrane protein. At least two prominent endothelial proteins have been reported to bind albumin, FcRn[30] and secreted protein acidic and rich in cysteine (SPARC or osteonectin)[31]. An albumin binding protein gp60 was previously reported but we could not identify it in our models on western blots.

FcRn is highly expressed in BBB endothelia where it binds and recycles both albumin and IgG back to the bloodstream[22]. Partial knockdown of FcRn in brain endothelial cells by two shRNAs resulted in a significant reduction (>80%, $p<0.0001$) in endothelial albumin endocytosis *in vitro* (Figure 4E-F and Supplementary Figure 5A-B). FcRn knockdown also reduced transcytosis of albumin in BTB cultures by ~37% (Figure 4G, $p=0.004$) without affecting paracellular permeability (Supplementary Figure 5C). Our data indicate that a major portion of albumin endocytosis and transcytosis in the BTB is not via nonselective macropinocytosis but involves an FcRn-mediated pathway.

Albumin macropinocytosis through the BTB displays features of CIE. We asked if albumin endocytosis, via FcRn binding, fit a general profile of CIE described for CD44 *in vitro*. Brain endothelial FcRn was N-glycosylated (Figure 5A), in agreement with previous data in rat kidney cells[32]. Brain endothelial FcRn bound Gal-3 in two-way co-immunoprecipitations (Figure 5B-C, input controls on Supplementary Figure 6) and in co-immunofluorescence experiments (Figure 5D). When Gal-3 was knocked down from brain endothelial cells using two shRNAs, albumin endocytosis was reduced by 80% ($p<0.0001$) (Figure 5E-G). A reduction in albumin endocytosis was also observed if membrane glycosphingolipids were depleted from endothelial cells using a Glucosylceramide synthase (GCS) inhibitor[33] (Figure 5H-I). Endocytosis of albumin was dynamin-independent (Supplementary Figure 7A-D) and dependent on cdc42 (Supplemental Figure 8A-B).

A feature of CIE, post-endocytosis, is the formation of tubular endocytic vesicles that sort cargo to different outcomes[29,34]. We asked whether *in vivo* evidence of elongated intracellular nanotubes could be found in metastases undergoing transcytosis *in vivo*. Figure 5J presents multiple electron micrographs of *in vivo* JIMT1-BR normal (BBB) and metastatic (BTB) endothelia. Vesicles were prominent in both BBB and BTB endothelia (pink arrows) as this is the major route of transport for nutrients. However, in each BTB specimen, and not in BBB

tissues, more elongated vesicular structures were found suggestive of sorting nanotubes (blue arrows).

SPARC is an extracellular matrix modifying protein made by brain endothelial cells with albumin binding properties[35]. shRNA knockdown of SPARC only heterogeneously decreased albumin endocytosis in two clones (Supplementary Figure 9A-B). SPARC was also non-glycosylated (Supplementary Figure 9C). These data eliminated SPARC from further consideration as an albumin CIE pathway.

Albumin CIE proteins in human brain metastases. Whether the albumin CIE transcytotic pathway is evident in human brain metastases is important for potential translational development. Initial studies were conducted with a limited number of frozen craniotomy specimens, suitable for IF. A specimen, representative of 4/9 examined, shows localization of collagen IV to identify BTB capillaries and colocalization of Gal-3. The adjacent section was stained for FcRn and also shows patchy colocalization, which could be consistent with its coalescence into membrane domains (Figure 6A).

Additional studies were performed by IHC using formalin-fixed, paraffin embedded craniotomy specimens from multiple cancer histologies. Staining for Gal-3 on capillary endothelial cells was found in 60% of breast cancer and 50% of ovarian cancer craniotomies but only 17% of lung cancer specimens (Figure 6B-C). Staining was intracellular, which could reflect synthesis or intracellular sorting and trafficking, and luminal, consistent with an extracellular glycocalyx/CIE structure. A single specimen contained a margin of uninvolved brain in which Gal-3 was less prominent (Figure 6D). In addition to brain metastasis endothelial cells, Gal-3 expression was quantified on cancer cells, neurons, glial cells and macrophages in craniotomies on a 0-3+ intensity scale (Figure 6E, Supplementary Figure 10). While mainly absent on brain cells, intense staining was seen in cancer cells. These data suggest that a drug delivery via the CIE pathway could also operate in tumor cells, but spare most normal brain neurons.

Discussion

The identification of novel molecular pathways whereby drugs can be delivered at efficacious concentrations to brain metastases is an important goal in neuro-oncology. This manuscript used albumin as a probe to identify a CIE transcytosis pathway that may be of value for translation. Among five known transcytotic pathways tested in two brain-tropic, hematogenous model systems, albumin exhibited the most prevalent distribution to brain metastases, and little to the uninvolved or normal brain parenchyma. Additional endpoints may be informative in this type of comparison, but our initial use of confocal microscopy at different magnifications and photographic exposures to identify the maximal expression pattern limited subsequent analytical analyses. Albumin distributed to virtually all metastatic colonies and micrometastases, the latter rarely permeated by paracellular permeability compounds. Thus, the pathway may have a metastasis preventive role. Albumin distribution was also independent of biocytin-TMR, a paracellular permeability probe. Its relative lack of permeation into normal or uninvolved brain parenchyma may offer the advantage of minimizing adverse effects to normal neuronal function.

An *in vitro* assay was used to study albumin transcytosis. Many *in vitro* models of the BBB and BTB have been reported, each with strengths and deficiencies[36]. Our assay was modified from a previously reported culture system that faithfully replicated *in vivo* paracellular distribution[24]. Enlarging the pores separating endothelia from pericytes allowed cell connections and transcytosis. Albumin endocytosed into endothelial cells and transcytosed past the pericytes into culture medium and astrocytes.

Albumin penetrated the BTB, at least in part, by a transcytotic mechanism with features of CIE. Albumin transcytosis through the BTB was inhibited by 80-95% by inhibitors of macropinocytosis, in agreement with earlier EM studies of the BBB demonstrating large vesicles[16,17]. This observation identified a fundamental conundrum: If albumin dissolved in the bloodstream is pinocytosed passes the brain endothelium into metastases by the non-selective macropinocytosis process, why don't drugs dissolved in the bloodstream demonstrate the same trend? This question forced the hypothesis that an albumin-selective form of macropinocytosis must exist. We demonstrate herein that albumin transcytosis shows features of CIE. CIE includes a diverse set of pathways and cargoes where endocytic pit formation is independent of clathrin or

caveolin. Albumin endocytosis/transcytosis of the BTB required binding to FcRn, that FcRn was N-glycosylated and bound Gal-3, and membrane glycosphingolipids, all in agreement with classic CIE data for CD44[29]. Sorting intracellular tubules were found in JIMT-1BR BTB specimens *in vivo*, consistent with this post-endocytic CIE sorting mechanism[37]. Gal-3 staining was found on BTB endothelia of breast and ovarian human craniotomy specimens.

Translational research to promote drug delivery to brain metastases could follow a number of facets of a CIE pathway: First, albumin could itself serve as a drug delivery vehicle. Albumin temporarily and unstably coats nanoparticles to increase their solubility and adsorption, such as nab-paclitaxel[38]. It also stably conjugates to peptides or drugs to improve their half-life or accumulation[39-41]. Stable incorporation of albumin into nanoparticles has resulted in limited distribution in the normal mouse brain, and enhanced distribution in glioma or metastatic cancer lesions[42,43]. Second, other CIE pathways may be concentrated and active in the BTB and serve as drug linkages. CIE cargoes include MHC class I, the GPI anchored protein CD59, immunoglobulin superfamily member CD166, integrin β1, and CD44 [29,44,45]. Third, the FcRn-based pathway may also be important for monoclonal antibody efficacy for brain metastases. Finally, another facet of CIE is the galectin lattice/glycocalyx, glycoproteins and proteoglycans that cover the luminal surface of brain endothelial cells. BBB capillaries have ~40% of the lumen occupied with glycocalyx, higher than pulmonary or cardiac capillaries, and the brain glycocalyx is degraded by common CNS diseases such as stroke[46]. Galectins bind glycosylated proteins and lipids to form a lattice. With regard to CNS malignancies, an *in vitro* BTB model suggested a breakdown in the endothelial glycocalyx at the site of tumor cell intravasation[47].

Acknowledgements

This project has been funded in whole or in part with Federal funds from the National Cancer Institute, National Institutes of Health, under Contract No. HHSN261201500003I. The content of this publication does not necessarily reflect the views or policies of the Department of Health and Human Services, nor does mention of trade names, commercial products, or organizations imply endorsement by the U.S. Government. The human tissue samples from France were provided by AP-HM tumor bank AC-2013-1786, BB-0033-00097.

Conflict of interest statement. The authors declare no potential conflicts of interest.

References:

1. Boire A, Brastianos PK, Garzia L, Valiente M. Brain metastasis. *Nature Reviews Cancer.* 2020; 20(1):4-11.
2. Boogerd W, Dalesio O, Bais EM, Vandersande JJ. Response of brain metastases from breast cancer to systemic chemotherapy. *Cancer.* 1992; 69(4):972-980.
3. Walbert T, Gilbert MR. The role of chemotherapy in the treatment of patients with brain metastases from solid tumors. *International Journal of Clinical Oncology.* 2009; 14(4):299-306.
4. Bachelot T, Romieu G, Campone M, et al. Lapatinib plus capecitabine in patients with previously untreated brain metastases from HER2-positive metastatic breast cancer (LANDSCAPE): a single-group phase 2 study. *Lancet Oncol.* 2013; 14(1):64-71.
5. Freedman RA, Gelman RS, Anders CK, et al. TBCRC 022: A Phase II Trial of Neratinib and Capecitabine for Patients With Human Epidermal Growth Factor Receptor 2-Positive Breast Cancer and Brain Metastases. *Journal of Clinical Oncology.* 2019; 37(13):1081-1089.
6. Lin NU, Borges V, Anders C, et al. Intracranial Efficacy and Survival With Tucatinib Plus Trastuzumab and Capecitabine for Previously Treated HER2-Positive Breast Cancer With Brain Metastases in the HER2CLIMB Trial. *Journal of Clinical Oncology.* 2020; 38(23):2610-2619.
7. Steeg PS. The blood-tumour barrier in cancer biology and therapy. *Nature Reviews Clinical Oncology.* 2021; 18(11):696-714.
8. Gril B, Wei D, Zimmer A, et al. A HER2 Antibody Drug Conjugate controls growth of breast cancer brain metastasis in hematogenous xenograft models, with heterogeneous blood-tumor barrier penetration unlinked to a passive marker. *Neuro-oncol.* 2020; 22(11):1625-1636.
9. Samala R, Thorsheim H, Goda S, et al. Vinorelbine delivery and efficacy in the MDA-MB-231BR preclinical model of brain metastases of breast cancer. *Mol. Pharmacol.* 2016; 33(12):2904-2919.
10. Taskar KS, Rudraraju V, Mittapalli RK, et al. Lapatinib Distribution in HER2 Overexpressing Experimental Brain Metastases of Breast Cancer. *Pharmaceutical Research.* 2012; 29(3):770-781.
11. Lockman PR, Mittapalli RK, Taskar KS, et al. Heterogeneous Blood-Tumor Barrier Permeability Determines Drug Efficacy in Experimental Brain Metastases of Breast Cancer. *Clinical Cancer Research.* 2010; 16(23):5664-5678.
12. Thomas FC, Taskar K, Rudraraju V, et al. Uptake of ANG1005, A Novel Paclitaxel Derivative, Through the Blood-Brain Barrier into Brain and Experimental Brain Metastases of Breast Cancer. *Pharmaceutical Research.* 2009; 26(11):2486-2494.
13. Terrell-Hall TB, Nounou MI, El-Amrawy F, Griffith JIG, Lockman PR. Trastuzumab distribution in an in-vivo and in-vitro model of brain metastases of breast cancer. *Oncotarget.* 2017; 8(48):83734-83744.
14. Johnsen KB, Burkhart A, Thomsen LB, Andresen TL, Moos T. Targeting the transferrin receptor for brain drug delivery. *Progress in Neurobiology.* 2019; 181:101665.
15. Kumthekar P, Tang SC, Brenner AJ, et al. ANG1005, a Brain-Penetrating Peptide-Drug Conjugate, Shows Activity in Patients with Breast Cancer with Leptomeningeal Carcinomatosis and Recurrent Brain Metastases. *Clinical Cancer Research.* 2020; 26(12):2789-2799.
16. Vorbrodt AW, Dobrogowska DH, Lossinsky AS. Ultrastructural study on the interaction of native and cationized albumin-gold complexes with mouse brain microvascular endothelium. *Journal of Neurocytology.* 1996; 25(11):645-657.
17. Vorbrodt AW, Trowbridge RS. Ultrastructural study of transcellular transport of native and cationized albumin in cultured sheep brain microvascular endothelium. *Journal of Neurocytology.* 1991; 20(12):998-1006.

18. Knowland D, Arac A, Sekiguchi KJ, et al. Stepwise Recruitment of Transcellular and Paracellular Pathways Underlies Blood-Brain Barrier Breakdown in Stroke. *Neuron.* 2014; 82(3):603-617.

19. Palmieri D, Bronder JL, Herring JM, et al. Her-2 overexpression increases the metastatic outgrowth of breast cancer cells in the brain. *Cancer Res.* 2007; 67(9):4190-4198.

20. Palmieri D, Duchnowska R, Woditschka S, et al. Profound Prevention of Experimental Brain Metastases of Breast Cancer by Temozolomide in an MGMT-Dependent Manner. *Clinical Cancer Research.* 2014; 20(10):2727-2739.

21. Gril B, Paranjape A, Woditschka S, et al. Reactive astrocytic S1P3 signaling modulates the blood-tumor barrier in brain metastases. *Nature Communications.* 2018; 9(1).

22. Pyzik M, Sand KMK, Hubbard JJ, Andersen JT, Sandlie I, Blumberg RS. The Neonatal Fc Receptor (FcRn): A Misnomer? *Front. Immunol.* 2019; 10:24.

23. Urdang ZD, Bills JL, Cahana DY, Muldoon LL, Neuwelt EA. Toll-like Receptor 4 Signaling and Downstream Neutrophilic Inflammation Mediate Endotoxemia-Enhanced Blood Labyrinth Barrier Trafficking. *Otology & Neurotology.* 2020; 41(1):123-132.

24. Gril B, Paranjape AN, Woditschka S, et al. Reactive astrocytic S1P3 signaling modulates the blood-tumor barrier in brain metastases. *Nature Communications.* 2018; 9(1).

25. Daneman R, Zhou L, Kebede AA, Barres BA. Pericytes are required for blood-brain barrier integrity during embryogenesis. *Nature.* 2010; 468(7323):562-U238.

26. Orlandi PA, Fishman PH. Filipin-dependent inhibition of cholera toxin: Evidence for toxin internalization and activation through caveolae-like domains. *Journal of Cell Biology.* 1998; 141(4):905-915.

27. Wang S, Sharma P, Schoenlein P, Ely B. A protein histidine kinase is involved in polar organelle development in Caulobacter crescentus. *Proc. Natl. Acad. Sci. USA.* 1993; 90:630-634.

28. Koivusalo M, Welch C, Hayashi H, et al. Amiloride inhibits macropinocytosis by lowering submembranous pH and preventing Rac1 and Cdc42 signaling (vol 188, pg 547, 2010). *Journal of Cell Biology.* 2010; 189(2).

29. Lakshminarayan R, Wunder C, Becken U, et al. Galectin-3 drives glycosphingolipid-dependent biogenesis of clathrin-independent carriers. *Nature Cell Biology.* 2014; 16(6):592-+.

30. Sand KMK, Bern M, Nilsen J, Noordzij HT, Sandlie I, Andersen JT. Unraveling the interaction between FcRn and albumin: opportunities for design of albumin-based therapeutics. *Front. Immunol.* 2015; 5:1-21.

31. Liddelow SA, Dziegielewska KM, Mollgard K, et al. SPARC/osteonectin, an endogenous mechanism for targeting albumin to the blood-cerebrospinal fluid interface during brain development. *European Journal of Neuroscience.* 2011; 34(7):1062-1073.

32. Kuo TT, de Muinck EJ, Claypool SM, et al. N-Glycan Moieties in Neonatal Fc Receptor Determine Steady-state Membrane Distribution and Directional Transport of IgG. *Journal of Biological Chemistry.* 2009; 284(13):8292-8300.

33. Alam S, Fedier A, Kohler RS, Jacob F. Glucosylceramide synthase inhibitors differentially affect expression of glycosphingolipids. *Glycobiology.* 2015; 25(4):351-356.

34. Nguyen NTK, Ohbayashi N, Kanaho Y, Funakoshi Y. TBC1D24 regulates recycling of clathrin-independent cargo proteins mediated by tubular recycling endosomes. *Biochemical and Biophysical Research Communications.* 2020; 528(1):220-226.

35. Tilling T, Korte D, Hoheisel D, Galla HJ. Basement membrane proteins influence brain capillary endothelial barrier function in vitro. *Journal of neurochemistry.* 1998; 71(3):1151-1157.

36. Helms HC, Abbott NJ, Burek M, et al. In vitro models of the blood-brain barrier: An overview of commonly used brain endothelial cell culture models and guidelines for their use. *Journal of Cerebral Blood Flow and Metabolism.* 2016; 36(5):862-890.

37. Villasenor R, Schilling M, Sundaresan J, Lutz Y, Collin L. Sorting Tubules Regulate Blood-Brain Barrier Transcytosis. *Cell Reports.* 2017; 21(11):3256-3270.

38. Gardner ER, Dahut WL, Scripture CD, et al. Randomized crossover pharmacokinetic study of solvent-based paclitaxel and nab-paclitaxel. *Clinical Cancer Research.* 2008; 14(13):4200-4205.

39. Elsadek B, Kratz F. Impact of albumin on drug delivery--new applications on the horizon. *J Control Release.* 2012; 157(1):4-28.

40. Liu Z, Chen, X. Simple bioconjugate chemistry serves great clinical advances: albumin as a versitile platform for diagnosis and precision therapy. *Chem. Soc. Rev.* 2016; 45.

41. Kratz F, Elsadek B. Clinical impact of serum proteins on drug delivery. *J Control Release.* 2012; 161(2):429-445.

42. Liang J, Gao C, Zhu Y, et al. Natural Brain Penetration Enhancer-Modified Albumin Nanoparticles for Glioma Targeting Delivery. *ACS Appl Mater Interfaces.* 2018; 10(36):30201-30213.

43. Wan X, Zheng XY, Pang XY, et al. Lapatinib-loaded human serum albumin nanoparticles for the prevention and treatment of triple-negative breast cancer metastasis to the brain. *Oncotarget.* 2016; 7(23):34038-34051.

44. Mathew MP, Donaldson JG. Glycosylation and glycan interactions can serve as extracellular machinery facilitating clathrin-independent endocytosis. *Traffic.* 2019; 20(4):295-300.

45. Johannes L, Billet A. Glycosylation and raft endocytosis in cancer. *Cancer Metastasis Rev.* 2020; 39(2):375-396.

46. Yang X, Chen Y, Zhou Y, et al. GPC5 suppresses lung cancer progression and metastasis via intracellular CTDSP1/AhR/ARNT signaling axis and extracellular exosome secretion. *Oncogene.* 2021; 40(25):4307-4323.

47. Beyer S, Blocki A, Cheung MCY, Wan ZHY, Mehrjou B, Kamm RD. Lectin Staining of Microvascular Glycocalyx in Microfluidic Cancer Cell Extravasation Assays. *Life.* 2021; 11(3):179.

Figure legends

Figure 1. Characteristics of Far-red albumin distribution in two models of experimental brain metastasis. (A) Mice bearing either 231-BR or JIMT1-BR metastases were injected iv with Far-red labeled albumin, which was circulated for a short (30 min-1h) or long (4-6h) period, followed by perfusion. Brains were sectioned and analyzed by confocal microscopy for the maximal extent of distribution in metastatic colonies (groups of metastatic lesions) and uninvolved brain; a similar experiment was performed on normal mice. (B) Percentage of metastatic lesions (or microscopic fields in normal mice) with each pattern of maximal albumin distribution. (C-D) Representative examples of diffuse albumin transcytosis in 231-BR (C) and JIMT1-BR (D). (E) Representative examples of endocytosis limited to capillaries, where albumin-laden vesicles are observed. (F) "Stitched" image of brain section with JIMT1-BR metastases demonstrating widespread delivery of albumin to tumor cells.

Figure 2. Far-red-Albumin distribution to metastatic colonies and micrometastases is independent of paracellular distribution. Mice with either 231-BR or JIMT1-BR metastases received iv Far-red-Albumin and Tomato Red Biocytin (Biocytin TMR), a marker of paracellular permeability; probes circulated for 60 and 10 min, respectively, followed by perfusion. All lesions in a brain section were analyzed for fluorescent uptake pattern, and an adjacent section was H&E stained to co-localize metastases. (A) Representative example. (B) Extent of albumin distribution. (C) Distribution pattern of albumin in metastatic colonies, (D) Representative photographs of three predominant classes of albumin and biocytin-TMR distribution. (E-F) Distribution patterns in metastatic colonies and micrometastases. Magnification bar, 200 µm, Panel A, 50. µm, Panel D.

Figure 3. An *in vitro* assay of BBB and BTB function that demonstrates albumin transcytosis. A-E. Comparison of cultures using 3 µm and 0.4 µm porous filters. (A) Experimental design. 50 µg/ml Albumin-Alexa Fluor™ 594 was applied to the top chamber and incubated for 30 min. (B) Albumin endocytosis into endothelial cells. (C) Confocal microscopy through a 3 µm filter from a completed BTB assay demonstrating invasive NG2+ pericyte processes. (D) Albumin transcytosis into the lower chamber culture medium (n=5). (E) Paracellular distribution of doxorubicin after 45 min incubation, into the lower chamber (n=3). (F, G) Albumin endocytosis into endothelial cells using 231-BR or JIMT1-BR cells (n=4) and its representative images. (H-I) Endocytosis into endothelial cells, showing vesicles. (H) Confocal images of endothelial layer of completed assay showing increased Rab11 in BTB cultures and colocalization with albumin. (I) Transcytosis of albumin to astrocytes in lower chamber. All experiments conducted at least four times. Statistical differences were calculated using One-way analysis of variance (ANOVA).

Figure 4. Albumin transcytosis uses macropinocytosis, but dependent on FcRn. (A-D) Using the *in vitro* assay of BTB function, inhibitors of endocytic pathways were applied 30 min before addition of 50 µg/ml Albumin-Alexa Fluor™ 488 for 30 min. Brain endothelial

endocytosis was quantified in cultures with 231-BR (A,C) or JIMT1-BR (B,D) tumor cells, respectively (n=6). Scale bar 20 µm. (E-G) Endothelial knockdown of FcRn disrupts albumin endocytosis and transcytosis. (E) FcRn was knocked down in mouse brain endothelial cells using two independent shRNAs; the FcRn band is the top of a doublet as indicated by an arrow. (F) Confocal images of albumin endocytosis into endothelial cells using 231-BR and JIMT1-BR cells; scale bar 10 µm, (G) Transcytosis measuring albumin fluorescence into the lower chamber (n=4). Statistical differences were calculated using One-way ANOVA.

Figure 5. Albumin transcytosis demonstrates features of clathrin-independent endocytosis (CIE). (A) FcRn content of a brain endothelial lysate was separated into glycosylated and non-glycosylated fractions using Concanavilin A. (B-C) Brain endothelial FcRn bound Gal-3 in two-way co-immunoprecipitations. (D) Co-immunofluorescence of FcRn and Gal-3 in cultured brain endothelial cells. (E-G) Gal-3 knockdown in brain endothelial cells. (E) Western blot. (F-G) Endothelial endocytosis of Green-albumin in 231-BR and JIMT1-BR cultures, respectively. (H-I) Endothelial endocytosis of albumin after treatment with 30 µM of PPMP (DL-threo-1-Phenyl-2-palmitoylamino-3-morpholino-1-propanol) for 1 h to deplete glycosphingolipids in 231-BR (H) and JIMT1-BR (I) cultures. All experiments were performed at least four times and statistical differences were calculated using One-way ANOVA. (J) Electron micrographs of JIMT1-BR metastases and sham-injected brain. In both tissues normal vesicles are observed (pink arrows). Blue arrows identify long endocytic vesicles seen only in BTB specimens, consistent with sorting endothelial tubules (blue arrows). Scale bar: 10 nm.

Figure 6. Gal-3 positivity is a consistent feature of the BTB of human brain metastases. (A) Co-immunofluorescence of a snap frozen brain metastasis of human breast cancer showing Gal-3 colocalization with BTB vessels outlined by collagen IV. In the adjacent section the same structures demonstrate colocalization with FcRn. (B-C) Gal-3 immunohistochemical staining of formalin-fixed, paraffin embedded resected human brain metastases. (B) Representative photographs of Gal-3 staining patterns, on the luminal surface of, or within the BTB (black arrows highlighting perivascular, endothelial and negative staining-left to right). (C) Percentage of craniotomy specimens from three cancer histologies expressing BTB endothelial Gal-3. (D) Single example of a craniotomy specimen with a border of uninvolved brain, which demonstrated less Gal-3 staining. (E) Gal-3 staining patterns of other components of brain metastases of breast cancer, expressed as a percentage of specimens with 0-3+ intensity staining (n=10). Scale bars: 50 µm.

Figure 1

A

Intracardiac

Metastasis formation

Inject iv Far-red-ligand

0.5-6h circulation, Perfuse, Necropsy

B

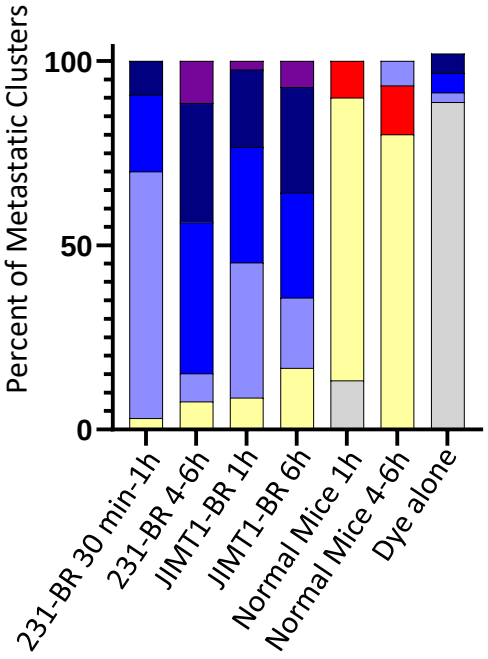

In both, higher in brain cells
In both, higher in mets
Diffusion in MME
Transcytosis in BTB
Endocytosis in BTB
In brain cells
Few foci or faint
Nothing

C

231-BR
Far-red-Albumin

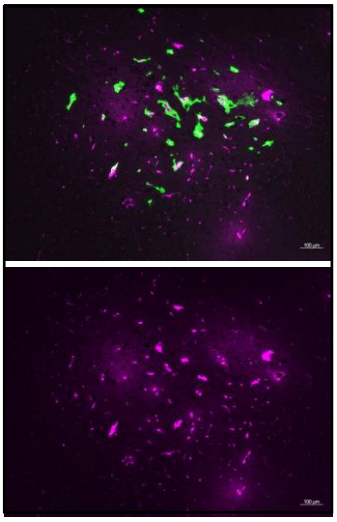

D

JIMT-1-BR
Far-red-Albumin

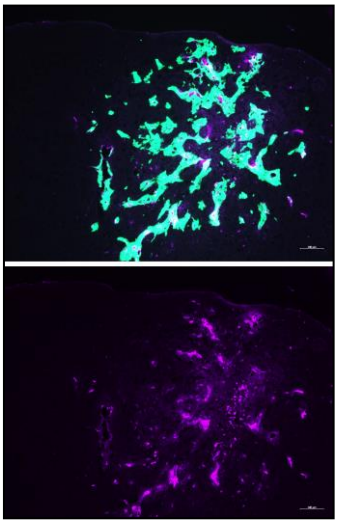

E

231-BR
Far-red-Albumin

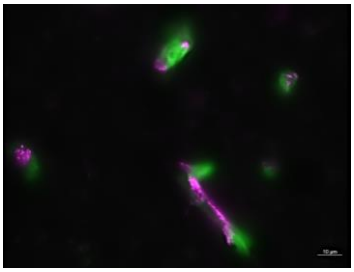

JIMT-1-BR
Far-red-Albumin

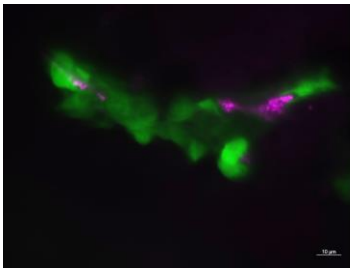

F

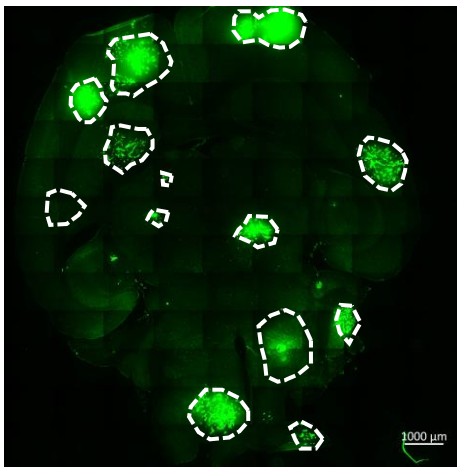

JIMT-1-BR

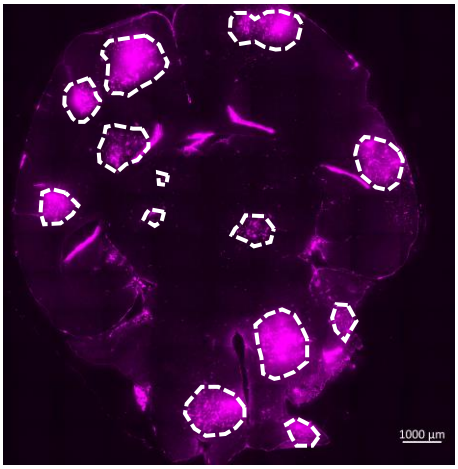

Far-red Albumin

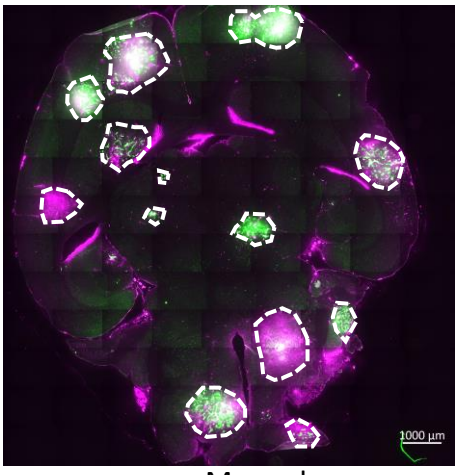

Merged

Figure 2

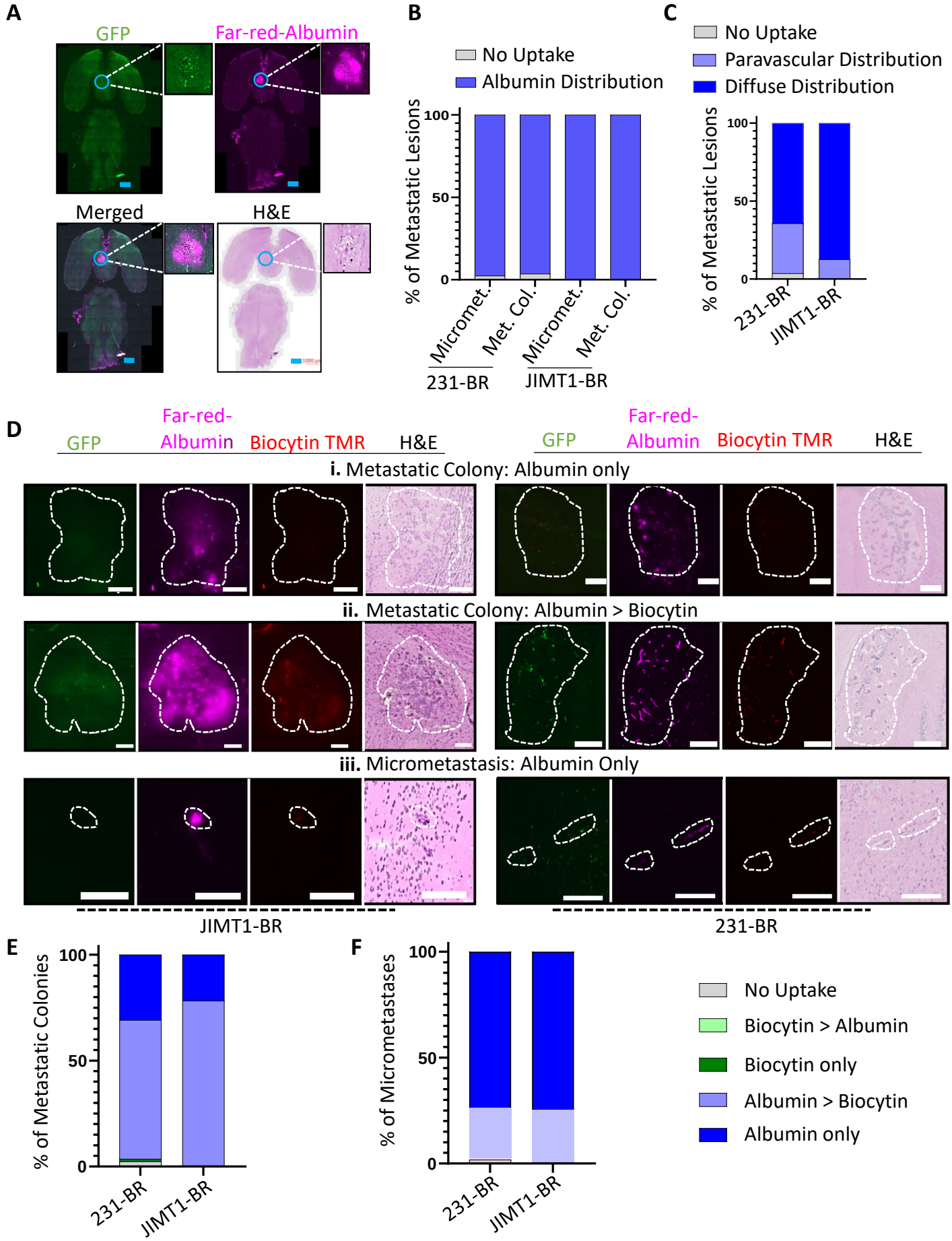
A
GFP
Far-red-Albumin
Merged
H&E
B
No Uptake
Albumin Distribution
% of Metastatic Lesions
100
50
0
Micromet.
Met. Col.
Micromet.
Met. Col.
231-BR
JIMT1-BR
C
No Uptake
Paravascular Distribution
Diffuse Distribution
% of Metastatic Lesions
100
50
0
231-BR
JIMT1-BR
D
GFP
Far-red-Albumin
Biocytin TMR
H&E
GFP
Far-red-Albumin
Biocytin TMR
H&E
i. Metastatic Colony: Albumin only
ii. Metastatic Colony: Albumin > Biocytin
iii. Micrometastasis: Albumin Only
JIMT1-BR
231-BR
E
% of Metastatic Colonies
100
50
0
231-BR
JIMT1-BR
F
% of Micrometastases
100
50
0
231-BR
JIMT1-BR
No Uptake
Biocytin > Albumin
Biocytin only
Albumin > Biocytin
Albumin only

Figure 3

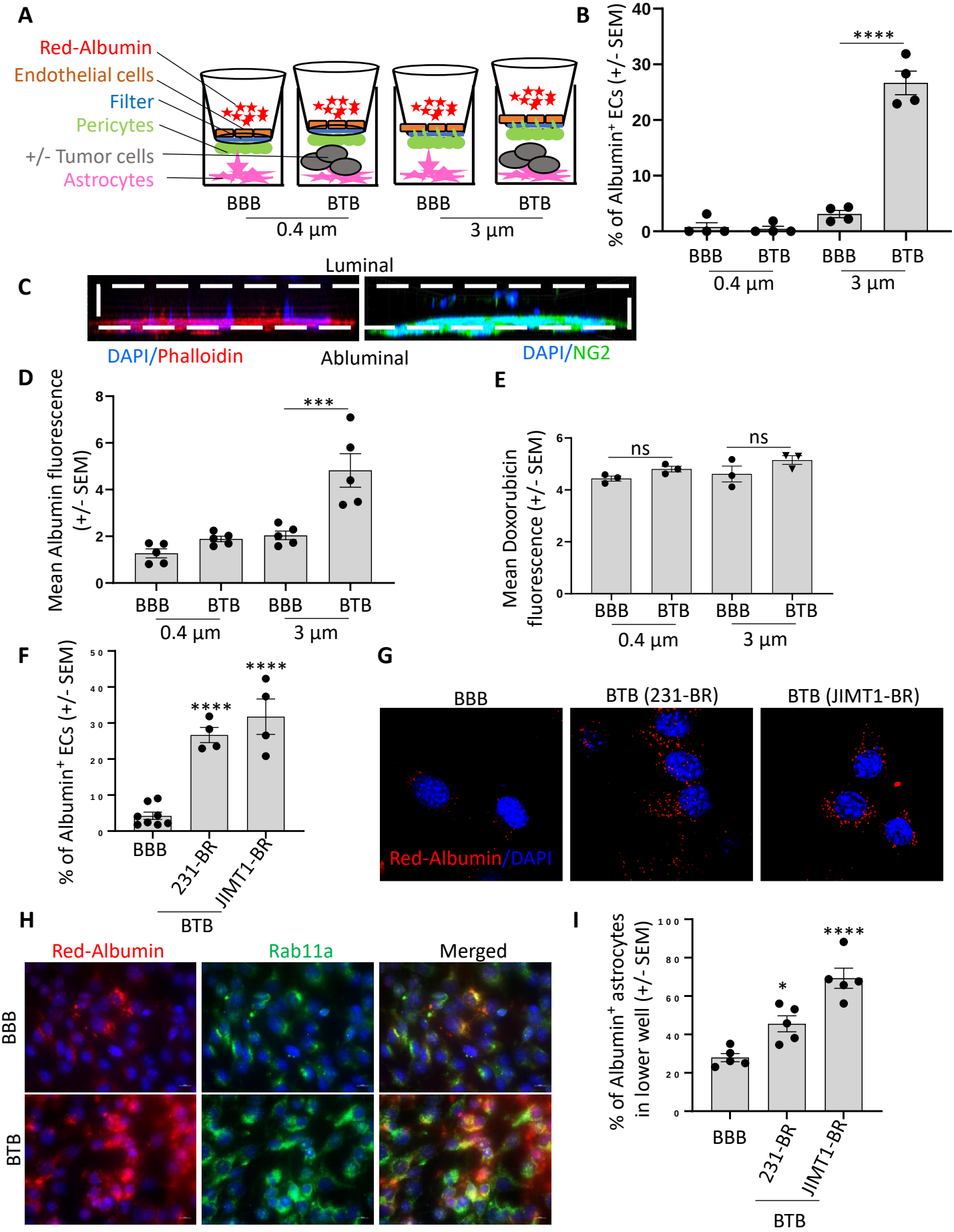
A
Red-Albumin
Endothelial cells
Filter
Pericytes
+/- Tumor cells
Astrocytes
BBB
BTB
BBB
BTB
0.4 µm
3 µm
B
% of Albumin+ ECs (+/- SEM)
****
BBB
BTB
BBB
BTB
0.4 µm
3 µm
C
Luminal
DAPI/Phalloidin
Abluminal
DAPI/NG2
D
Mean Albumin fluorescence (+/- SEM)
***
BBB
BTB
BBB
BTB
0.4 µm
3 µm
E
Mean Doxorubicin fluorescence (+/- SEM)
ns
ns
BBB
BTB
BBB
BTB
0.4 µm
3 µm
F
% of Albumin+ ECs (+/- SEM)
****
****
BBB
231-BR
JIMT1-BR
BTB
G
BBB
BTB (231-BR)
BTB (JIMT1-BR)
Red-Albumin/DAPI
H
Red-Albumin
Rab11a
Merged
BBB
BTB
I
% of Albumin+ astrocytes in lower well (+/- SEM)
*
****
BBB
231-BR
JIMT1-BR
BTB

Figure 4

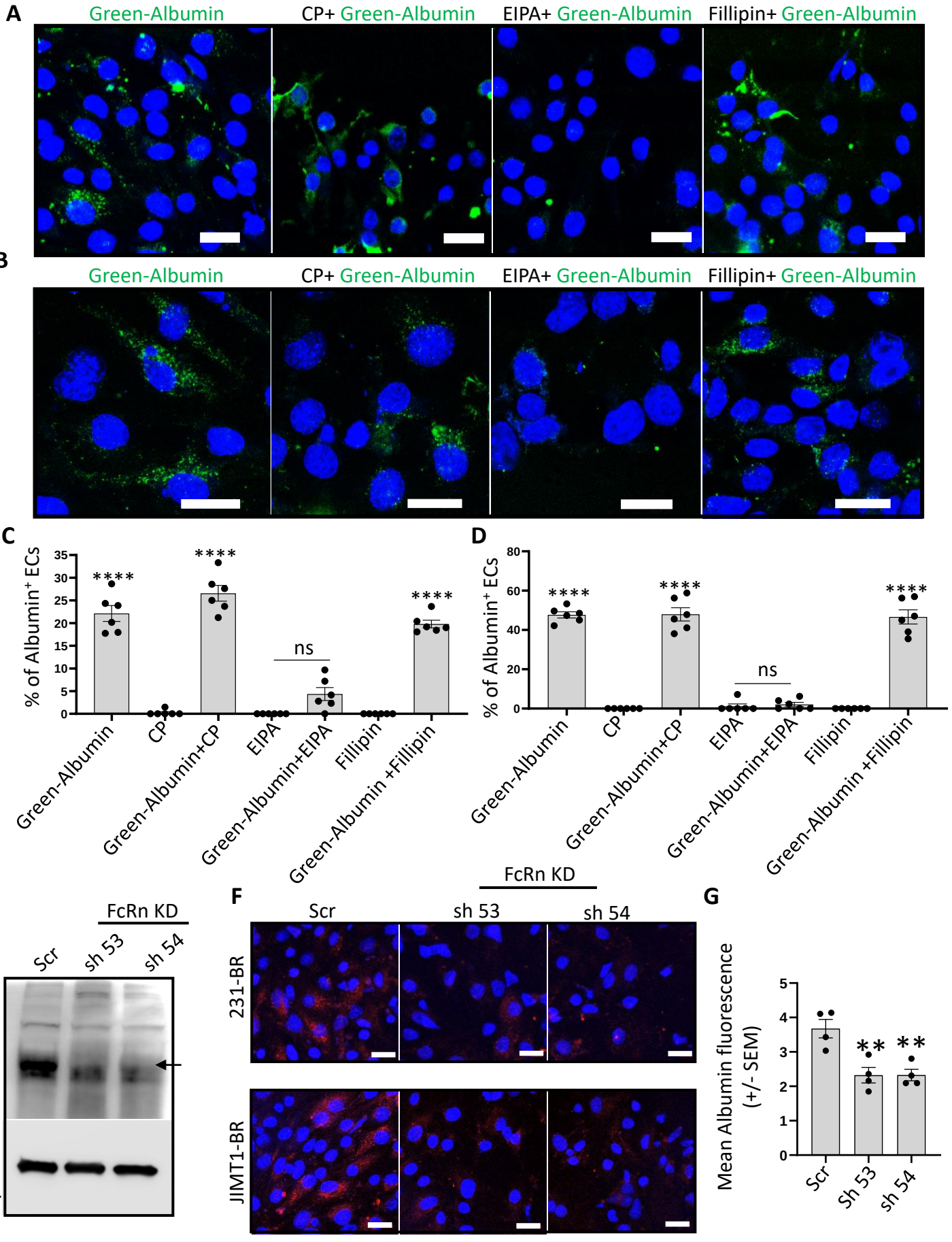
A
Green-Albumin
CP+ Green-Albumin
EIPA+ Green-Albumin
Fillipin+ Green-Albumin
B
Green-Albumin
CP+ Green-Albumin
EIPA+ Green-Albumin
Fillipin+ Green-Albumin
C
% of Albumin+ ECs
****
****
ns
****
Green-Albumin
CP
Green-Albumin+CP
EIPA
Green-Albumin+EIPA
Fillipin
Green-Albumin +Fillipin
D
% of Albumin+ ECs
****
****
ns
****
Green-Albumin
CP
Green-Albumin+CP
EIPA
Green-Albumin+EIPA
Fillipin
Green-Albumin +Fillipin
E
FcRn KD
Scr
sh 53
sh 54
FcRn
β-Actin
F
FcRn KD
Scr
sh 53
sh 54
231-BR
JIMT1-BR
G
Mean Albumin fluorescence (+/- SEM)
**
**
Scr
Sh 53
sh 54

Figure 5

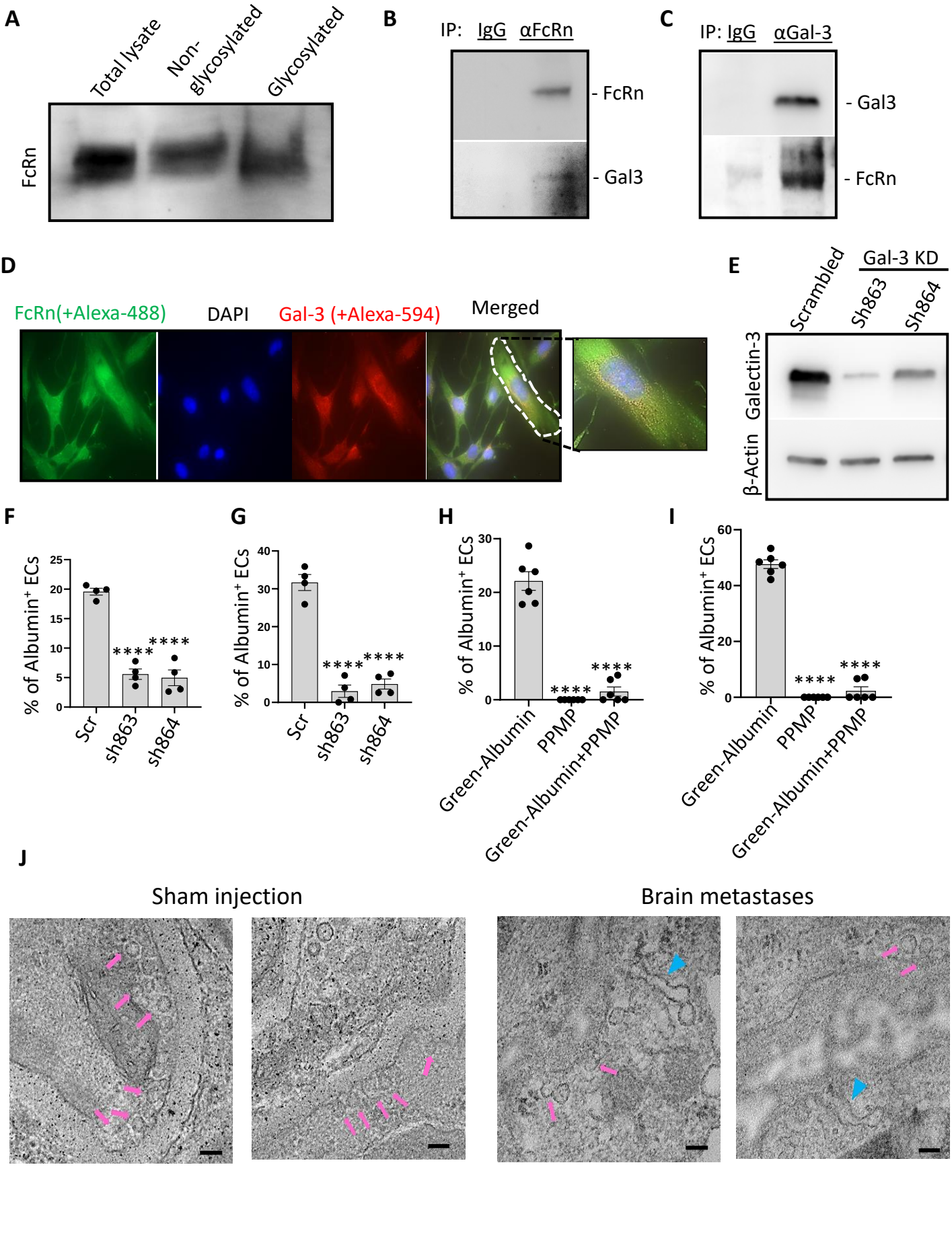
A
Total lysate
Non-glycosylated
Glycosylated
FcRn
B
IP: IgG αFcRn
- FcRn
- Gal3
C
IP: IgG αGal-3
- Gal3
- FcRn
D
FcRn(+Alexa-488)
DAPI
Gal-3 (+Alexa-594)
Merged
E
Scrambled
Gal-3 KD
Sh863
Sh864
Galectin-3
β-Actin
F
% of Albumin+ ECs
Scr
sh863
sh864
G
% of Albumin+ ECs
Scr
sh863
sh864
H
% of Albumin+ ECs
Green-Albumin
PPMP
Green-Albumin+PPMP
I
% of Albumin+ ECs
Green-Albumin
PPMP
Green-Albumin+PPMP
J
Sham injection
Brain metastases

Figure 6

A

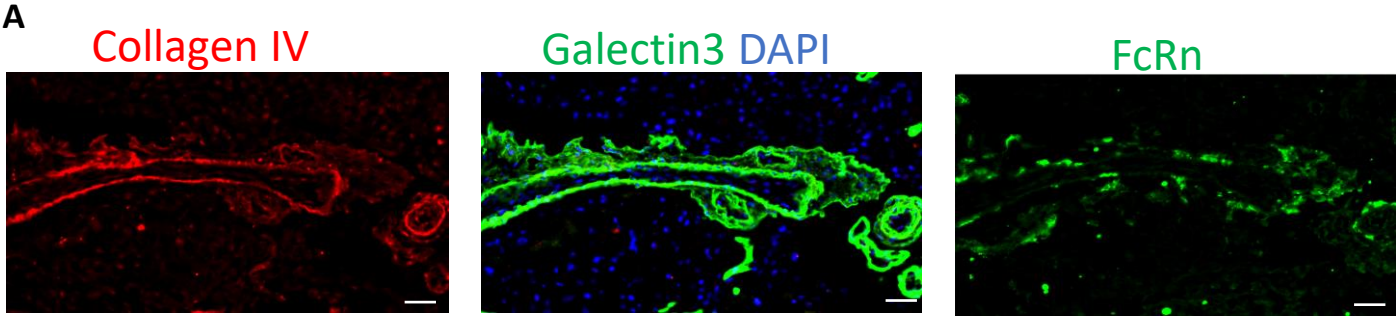

B

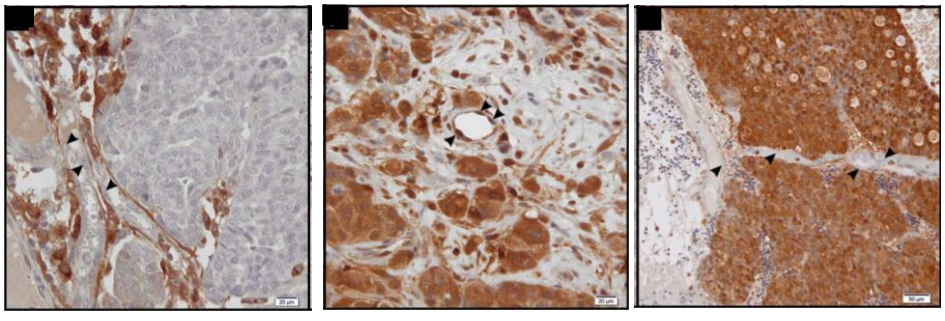

Perivascular staining | Endothelial staining | Negative

C

Histology:	Fraction (%) Specimens with Endothelial Positivity:
Breast	6/10 (60%)
Ovarian	6/12 (50%)
Lung	2/12 (17%)

D

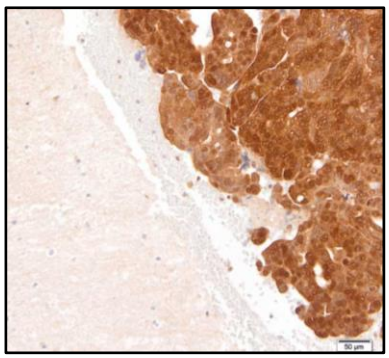

E